

Base Hydrolysis of Methyltrioxorhenium. The Mechanism Revised and Extended: A Novel Application of Electrospray Mass Spectrometry

James H. Espenson,* Haisong Tan, Sahana Mollah, R. S. Houk, and Matthew D. Eager

The Ames Laboratory and Department of Chemistry, Iowa State University, Ames, Iowa 50011

Received April 20, 1998

The full kinetic pH profile for the base-promoted decomposition of MTO to CH_4 and ReO_4^- was examined with the inclusion of new data at pH 7–10. Spectroscopic and kinetic data gave evidence for mono- and dihydroxo complexes: $\text{MTO}(\text{OH}^-)$ and $\text{MTO}(\text{OH}^-)_2$. Parallel unimolecular eliminations of methane from these species account for the rate–pH profile; the respective rate constants are $\text{MTO}(\text{OH}^-)$, $k = 4.56 \times 10^{-5} \text{ s}^{-1}$ and $\text{MTO}(\text{OH}^-)_2$, $k = 2.29 \times 10^{-4} \text{ s}^{-1}$ at 25 °C. Some kinetic data were acquired with electrospray mass spectrometry to monitor the buildup in the concentration of perhenate ions. Reliable signals for each of the isotopomers of ReO_4^- were obtained by this method with initial MTO concentrations of 160 μM .

Introduction

The base hydrolysis kinetics of methyltrioxorhenium ($\text{CH}_3\text{-ReO}_3$, abbreviated as MTO) was reported by two groups of workers in 1996.^{1,2} Both groups, agreeing that the exclusive products are methane and perhenate ions, wrote this chemical equation for the net reaction:



The pH ranges of the two investigations were, however, widely separated, approximately 3–6¹ and 11–14.² Neither set of data can correctly be extrapolated to the intermediate pH region while also supporting the independent claims as to mechanism. The dilemma in the kinetics is clearly apparent from the two pieces of the experimental pH profile, shown in Figure 1. Both sets of data are shown as solid lines within the pH region actually measured, using the analytical expressions for the rate constants to construct these curves. Additionally, the rate law from each set of experiments was then extrapolated toward neutral pH, outside the range of measurement, by the mathematical forms given in the respective reports. The extrapolated curves diverge widely. Both interpretations cannot be as stated: the rate constants thus assigned could not be reconciled with one another, in that they differ by more than 4 orders of magnitude. Expressed as the value of k in the equation $v = k[\text{MTO}][\text{OH}^-]$, the respective values of k are $8.6 \times 10^2 \text{ L mol}^{-1} \text{ s}^{-1}$ (extrapolated to 298 K)¹ vs $2.7 \times 10^{-2} \text{ L mol}^{-1} \text{ s}^{-1}$.² Neither set of data necessarily disagrees with the other, however, if a more refined model can be formulated on the basis of kinetics in the intermediate pH range. The goal of this study has been to obtain kinetic data that cover the full pH range and to formulate a single mechanism to describe all the data.

The reaction kinetics has now been studied at intermediate pH values, with UV–vis and electrospray mass spectrometric (ES-MS) techniques. The ES-MS technique is widely used for

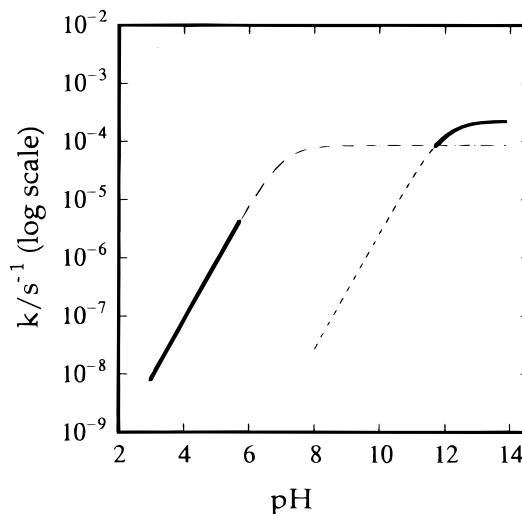


Figure 1. The pH profiles for two sets of kinetic data for the OH^- -induced decomposition of MTO. One set used data for pH 2.97–5.70, extrapolated to 25 °C,¹ the other set refers to measurements over the range 11.7–13.8. Each is shown as a bold line. Each set of data was extrapolated by the chemical and algebraic model given in the respective publication, with the extrapolated portions shown as dashed lines.

the determination of the molecular weights and structures of large biological molecules.^{3,4} This technique has also been used for the determination of many inorganic species, from ion clusters to bare metal ions.^{5–10} To date, applications of the ES-MS method to kinetics problems have, however, been relatively rare.⁷

- (1) Laurenczy, G.; Lukács, F.; Roulet, R.; Herrmann, W. A.; Fischer, R. W. *Organometallics* **1996**, *15*, 848–851.
- (2) Abu-Omar, M.; Hansen, P. J.; Espenson, J. H. *J. Am. Chem. Soc.* **1996**, *118*, 4966–4974.
- (3) Fenn, J. B.; Mann, M.; Meng, C. K.; Wong, S. F.; Whitehouse, C. M. *Science* **1989**, *246*, 46.

- (4) Smith, R. D.; Loo, J. A.; Edmonds, C. G.; Barinaga, C. J.; Udseth, H. R. *Anal. Chem.* **1990**, *62*, 882.
- (5) Colton, R.; D'Agostino, A.; Traeger, J. C. *Mass Spectrom. Rev.* **1995**, *14*, 79.
- (6) Corr, J. J.; Anacleto, J. F. *Anal. Chem.* **1996**, *68*, 2155.
- (7) Charbonniere, L. J.; Williams, A. F.; Frey, U.; Merbach, A. E.; Kamalaprija, P.; Schaad, O. *J. Am. Chem. Soc.* **1997**, *119*, 2488–2496.
- (8) Blades, A. T.; Jayaweera, P.; Ikonou, M. G.; Kebarle, P. *J. Chem. Phys.* **1990**, *92*, 5900.
- (9) Blades, A. T.; Ho, Y.; Kebarle, P. J. *J. Phys. Chem.* **1996**, *100*, 2443.
- (10) Klassen, J. S.; Kebarle, P. J. *J. Am. Chem. Soc.* **1996**, *118*, 12437.

Table 1. Typical ES-MS Operating Conditions

sample flow rate	17 $\mu\text{L min}^{-1}$
nebulizer gas, pressure	nitrogen, 280 kPa
curtain gas, back-pressure, temperature	nitrogen (ultrapure carrier grade), 550 kPa, 45 $^{\circ}\text{C}$
ionization needle voltage (V_{ISV})	−4400 V
interface plate voltage (V_{IN})	−450 V
orifice plate voltage (V_{OR})	−130 V
RF only quadrupole voltage (V_{RO})	−100 V
mass analyzer quadrupole voltage (V_{RI})	−95 V
CEM detector voltage	2500 V
operating pressure of quadrupole chamber	4.0 mPa

Experimental Section

Materials. The solutions for kinetics were prepared using high-purity water obtained by passing laboratory distilled water through a Millipore-Q water purification system. HPLC-grade acetonitrile (Fisher Scientific) was used in the ES-MS measurements. MTO, sodium perrhenate, sodium *p*-toluenesulfonate (= tosylate), sodium carbonate, and potassium phosphate were used as received.

Instrumentation. UV–vis spectra were obtained from a Shimadzu UV-3101PC instrument. A Perkin-Elmer SCIEX API-1 mass spectrometer was used for the ES-MS study. Typical conditions used in the operation of the ES-MS instrumentation are summarized in Table 1. The voltages were optimized to maximize the signal for the species of interest. Peak hopping data were collected using a 100-ms dwell time. Spectral scans were collected by adding 10 consecutive scans together using a dwell time of 10 ms per 0.1 amu.

Kinetics. All of the kinetics determinations, by the UV and ES-MS methods, were carried out in aqueous solution at 25.0 ± 0.5 $^{\circ}\text{C}$. A 5 cm quartz cuvette was used, and the starting concentration of MTO was 1.60×10^{-4} M (40 ppm). Other concentrations were 3.09×10^{-5} M (6 ppm) sodium tosylate, and 1–20 mM buffer solution. The solution was diluted with an equal volume of acetonitrile just before the ES-MS measurement. The addition of an organic solvent greatly enhances the ion signal in ES-MS. The actual kinetics data apply, however, to a strictly aqueous medium. The buffers used for the different pH ranges were 4.5–6.0, HOAc/NaOAc; 6.5–8.0, $\text{KH}_2\text{PO}_4/\text{K}_2\text{HPO}_4$; and 8.0–10.5, $\text{NaHCO}_3/\text{Na}_2\text{CO}_3$. Above pH 10.5, NaOH alone determined the pH. The ionic strength change proved to have little influence on the rate constants.

Results

Kinetics. As will be shown, data in the intermediate pH region do define an approximate plateau between the limiting values of the earlier studies, although the rate constants are not those that would have been extrapolated from either of the previous experimental studies. We can now propose a mechanism to account for the kinetic data over the entire pH range.

The decomposition of MTO to perrhenate ions was followed at several UV wavelengths. Some reactions were followed by monitoring the absorbance as a function of time at a fixed wavelength; the readings would rise or fall with time depending on the relative values of the molar absorptivities of MTO and ReO_4^- at the chosen wavelength. Other experiments were based on repetitive UV scans over time. In one treatment, these files were analyzed by extracting absorbance values at a given wavelength. In both of these cases the rate constant was obtained by nonlinear least-squares fits to a first-order rate equation: $\text{Abs}_t = \text{Abs}_{\infty} + (\text{Abs}_0 - \text{Abs}_{\infty}) \times \exp(-kt)$. The single-wavelength data were of greater precision, however, and were used in this analysis.

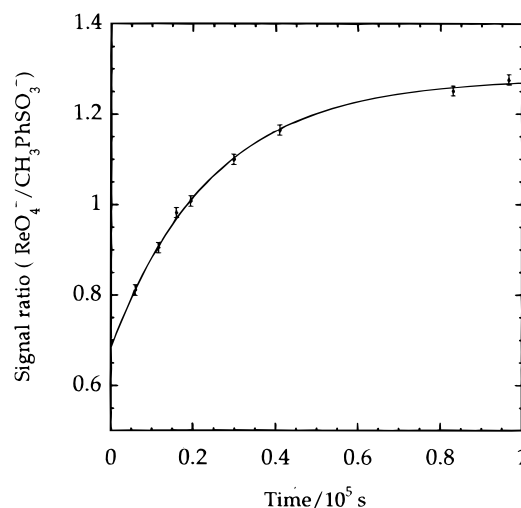


Figure 2. Typical plot of the signal ratio for $\text{ReO}_4^-/\text{TsO}^-$ vs time obtained in an ES-MS experiment. The initial concentration of MTO was 160 μM and the pH was buffered at 8.0. The curve shown corresponds to one of the two isotopes of rhenium. The curves through the points are the first-order kinetic fits.

ES-MS has been used for the determination of many inorganic ions both qualitatively and quantitatively.¹¹ We have found that the perrhenate anion gives a clean mass spectrum in 1:1 $\text{CH}_3\text{CN}:\text{H}_2\text{O}$ solution under ES-MS conditions. The only two significant peaks are those for the two isotopes, ^{185}Re and ^{187}Re , with natural abundances of 37.07 and 62.93%, respectively.¹² Thus ReO_4^- shows peaks at m/z 249 and 251 in a relative abundance of 1:1.7. Using the tosylate anion (m/z 171) as the internal standard for concentration, we were able to monitor the increase in intensity of each of the perrhenate peaks with time as the reaction proceeded at pH 7–10.

Figure 2 shows the change in the perrhenate signal at m/z 251, relative to tosylate, as a function of time. The time to collect the mass spectral data was ~ 100 s, which is much smaller than the reaction time, typically $\sim 10^4$ s. The intensity–time data gave excellent fits to first-order kinetics. The errors shown represent the standard deviations estimated from counting statistics based on total counts observed for each species.

To determine the absolute conversion in the decomposition reaction, the method of standard additions was applied. Under the same ES-MS conditions, increments of a sodium perrhenate solution were added to the reaction vessel at concentrations 4–16 ppm in total. This was done to spent reaction solutions at pH 7 and 10. Figure S1 (Supporting Information) shows this result at pH 10. There is a nearly linear increase of the intensity ratio with the concentration of the added perrhenate ions. If this line is extrapolated linearly to the abscissa, its intercept corresponds to a value of 22 ppm of ReO_4^- . This is only slightly higher than that of the nominal value of 20 ppm, which could be due to the volume contraction upon mixing water and acetonitrile.

pH Variation. The various buffers listed previously were used to set $[\text{OH}^-]$ in different experiments in the pH range 5–11. Since MTO was present in the range $(1-2) \times 10^{-4}$ M, much lower than the buffer capacity, the pH could be taken as nearly constant in each experiment. The new kinetic data, from UV and ES-MS, along with the experimental data at low pH¹ and high pH,² were used to create a new pH profile, given in Figure 3.

(11) Guizdala, A. B., III; Johnson, S. K.; Mollah, S.; Houk, R. S. *Anal. Atom. Spectro.* **1997**, *12*, 503.

(12) Friedlander, G.; Kennedy, J. W. *Nuclear and Radiochemistry*; John Wiley & Sons: New York, 1955; p 434.

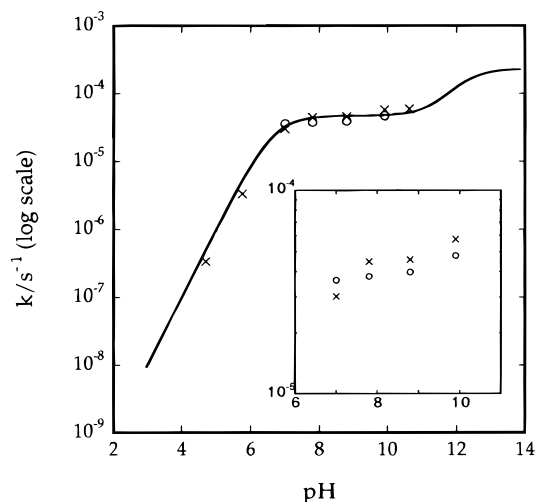


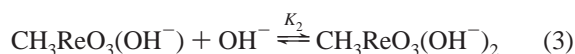
Figure 3. Variation of the observed rate constant with pH, including the new values at intermediate pH, shown as ○ (ES-MS) and × (UV-vis). The solid curve is the fit of all data to eq 6. The inset expands the middle region.

Interpretation and Discussion

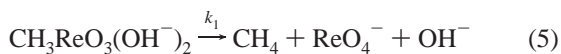
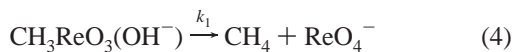
Mechanisms. The pH profile shows two rising portions and two plateaus, as if the data represented the titration curves for the formation of two intermediates. Indeed, this concept provides the basis for one of the mechanisms that can be drawn to account for the pH profile. The acidity of MTO (pK_a 7.5)^{13,14} has been recognized, which we find convenient to write as the complexation of OH^- :



If the second, high-pH plateau is to be accounted for in an analogous manner, then a second equilibrium, eq 3, must be written:



If this is the model, then each species must react independently at the unimolecular rate given by its plateau. The chemical equations are as shown in eqs 4 and 5



The smooth curve in Figure 3 is the pH profile for the fit of the rate constants to this model, as expressed in eq 6

$$k = \frac{k_1 K_1 [OH^-] + k_2 K_1 K_2 [OH^-]^2}{1 + K_1 [OH^-] + K_1 K_2 [OH^-]^2} \quad (6)$$

In the low-pH region, the rate is $k_1 K_1 [OH^-]$, in agreement with the form reported.¹ In the limit of very high pH, the rate will be given by $k_2 K_2 [OH^-]/(1 + K_2 [OH^-])$, also consistent with the form reported.²

The data over the entire pH range were fitted by eq 6 using the method of nonlinear least-squares regression, and the four

parameters were deduced without reference to values reported previously. The fitted values of the parameters are

$$k_1 = (4.56 \pm 0.20) \times 10^{-5} \text{ s}^{-1}$$

$$K_1 = (2.5 \pm 0.9) \times 10^7 \text{ L mol}^{-1}$$

$$k_2 = (2.29 \pm 0.03) \times 10^{-4} \text{ s}^{-1}$$

$$K_2 = 73.1 \pm 5.6 \text{ L mol}^{-1}$$

Let us now examine what comparisons can be made on the basis of these values. The value of K_1 affords $pK_{a1} = 6.70$, perhaps acceptably close to the reported 7.5, given the different methods employed. From K_2 and $pK_w = 14$, $pK_{a2} = 12.2$ for $MTO(OH^-) + H_2O = MTO(OH^-)_2 + H^+$; this compares favorably with the reported value,² $pK_a = 11.9$ (kinetics) and 11.7 (UV titration) under alkaline conditions. Of course the symbolism used in this work is different than that in ref 2, and this constant is not labeled the same there as it appears here.

From the calculated product $k_1 K_1$, we have the apparent bimolecular rate constant for the reaction of $MTO + OH^-$ in the acidic region: $1.03 \times 10^3 \text{ L mol}^{-1} \text{ s}^{-1}$, compared to $0.86 \times 10^3 \text{ L mol}^{-1} \text{ s}^{-1}$, calculated from the kinetic data and the value of K_1 . The difference is not large and can be traced to the ways in which pK_{a1} was treated.

What is one to make of the unimolecular constants cited above: $k_1 = (4.56 \pm 0.20) \times 10^{-5} \text{ s}^{-1}$ and $k_2 = (2.29 \pm 0.03) \times 10^{-4} \text{ s}^{-1}$? The two are similar to one another, being separated by a factor of only 5. In contrast, MTO itself shows no tendency to produce methane. These findings imply that the reaction occurs by the elimination of methane from the methyl group and the proton of the coordinated hydroxide. Whether one OH^- group or two are coordinated to rhenium makes rather little difference; at most, the second hydroxide facilitates methane release by making the incipient perrhenate ion into a better leaving group.

Independent evidence has been obtained for each of the hydroxo-MTO anions. The bright yellow $[MTO(OH)_2]^-$ was detected spectrophotometrically and is also evident from pH measurements.^{13,14} The UV-vis spectra of MTO remains the same between pH 1 and 6, whereas it changes above pH ~6 and ~11. These findings and the shape of the pH titration curve provide support for the species $[MTO(OH)]^-$ and $[MTO(OH)_2]^{2-}$.

The electrospray conditions that produced strong signals for perrhenate and tosylate ions did not show the presence of $[MTO(OH)]^-$ or $[MTO(OH)_2]^{2-}$. This at first appeared alarming, since $[MTO(OH)]^-$ should be present at a significant concentration at pH 8–11 according to our analysis, Figure S2 (Supporting Information). When the voltage difference between the skimmer and the RF-only quadrupole rods was reduced from 30 to 3 V, weak peaks of $[MTO(OH) \cdot 4H_2O]^-$ became evident in the spectrum at pH 11 in a carbonate buffer. Apparently, collision conditions that are energetic enough to strip solvent molecules from $[MTO(OH) \cdot 4H_2O]^-$ also cause it to disproportionate. This solvated anion would have been missed had the measurements been restricted to a single collision energy, illustrating the importance of examining the effect of collision conditions on electrospray spectra of inorganic and organometallic ions before concluding the certain species are absent from the sample, as noted by others.^{5,8–10}

The secondary solvation of this anion was found under these conditions, because of the low energy used. A further finding emerged: an additional peak corresponding in mass to “ $MeReO_5^-$ ” was seen but only in carbonate buffer. The point

(13) Herrmann, W. A.; Fischer, R. W.; Scherer, W. *Adv. Mater.* **1992**, *4*, 653.

(14) Herrmann, W. A.; Fischer, R. W. *J. Am. Chem. Soc.* **1995**, *117*, 3223.

was not investigated further; perhaps in alkaline solution MTO catalyzes the conversion of CO_3^{2-} to CO_2 .

Figure S2 shows the constructed speciation diagram for MTO and its hydroxo complexes, calculated from the best-fit values of K_1 and K_2 . Recognition of the species present over the entire range allows the formulation of a satisfactory mechanism.

This appears to be one of the early applications, and perhaps the first, of the ES-MS technique to a kinetics problem in inorganic or organometallic chemistry. The exceptional sensitivity of the method should commend it for many applications.

Acknowledgment. This research was supported by the U.S. Department of Energy, Office of Basic Energy Sciences, Division of Chemical Sciences under Contract W-7405-Eng-82.

Supporting Information Available: Two figures depict the calibration of the MS-ES data by standard additions and the speciation of MTO as a function of hydroxide ion concentration (2 pages). Ordering information is given on any current masthead page.

IC980447X